UCM-17/3

Clustering resonance effects in the electronic energy spectrum of tridiagonal Fibonacci quasicrystals.

Enrique Maciá

Dpto. Física de Materiales, Facultad CC. Físicas,

Universidad Complutense de Madrid, E-28040, Spain

(Dated: May 19, 2017)

Abstract

In this work we show that the fundamental structure of the electronic energy spectrum of binary Fibonacci quasicrystals can be decomposed in terms of two main contributions, stemming from two related characteristic symmetries. The algebraic approach we introduce allows us for a unified and systematic description of the energy spectrum finer structure details in terms of block matrices commutators properties, within the framework of a renormalization approach based on transfer matrices. Close analytical expressions can be explicitly obtained by exploiting some algebraic properties of these blocks commutators. In particular, the overall main features of the electronic energy spectrum structure are related to the roots of a series of polynomials of the form $p_{F_j}(E)$, where the subscript denotes the degree of the polynomial, which is given by a Fibonacci number F_j. These polynomials, in turn, are derived in a systematic way from commutators involving progressively longer palindromic fundamental blocks containing two types of basic renormalized matrices. In this way, we can classify the resonance energies defining the different fragmentation patterns of the energy spectrum on the basis of purely algebraic criteria. *The transmission coefficient of these resonant states is always bounded below, although their related Landauer conductance values may range from highly conductive to highly resistive ones, depending on the system length.* The obtained results significantly contribute to gain a better understanding of the symmetry principles governing the fragmentation process leading to the characteristic nested structure of the energy spectrum.

Keywords: Quasicrystals, Fibonacci, energy spectrum structure, transfer matrix based renormalization

INTRODUCTION

Quasicrystalline alloys provide an intriguing example of ordered solids made of typical metallic atoms which do not exhibit most of the physical properties usually signaling the presence of metallic bonding. In fact, quasicrystals (QCs) remarkably depart from standard metallic behaviour and, attending to their electrical transport properties, thermodynamically stable QCs of high structural quality resemble a more semiconductor-like than metallic character.[1–5] A growing number of both experimental measurements and numerical simulation results suggest that a main factor determining the remarkable properties of both decagonal and icosahedral QCs might be related to physicochemical aspects involving nearest and next-nearest atomic neighbours, thereby highlighting the important role of chemical bonding in the emergence of some specific physical properties of QCs.[6–10] In actual QCs the bonding network extends throughout the three dimensions of physical space, resulting in an involved quasiperiodic distribution of atoms and bonds which renders the full-fledged problem not amenable to analytical treatment.[11] Accordingly, as a first approximation we will consider a suitable one-dimensional model system able to account for the role of a quasiperiodic pattern of both atoms *and* chemical bonds in the resulting electronic structure in the simplest possible manner.

Previous studies have demonstrated that several characteristic physical properties of one-dimensional quasiperiodic lattices, like the fractal structure of their energy spectra and their related eigenstates, can be understood in terms of resonance effects involving a relatively small number of atomic clusters of progressively increasing size. In most of these works this scenario has been discussed in terms of real-space based renormalization group approaches considering either the mathematically simpler, but chemically unrealistic, diagonal (different types of atoms connected by the same type of bond) and off-diagonal (the same type of atom but different types of bonds between them) models.[12–19] Relatively fewer works have been addressed to the mathematically more complex general case in which both diagonal and off-diagonal terms are present in the model Hamiltonian.[20–27]

Since the properties of a chemical bond linking two different atoms generally depend on their chemical nature, any realistic treatment must explicitly consider that the aperiodic sequence of atoms along the chain naturally induces an aperiodic sequence of bonds in the considered alloy. Accordingly, in this work we will study the structure of the electronic

energy spectrum of Fibonacci quasicrystals (FQCs) characterized by the presence of both atomic and chemical bonding quasiperiodic distributions, which are described by means of a tridiagonal Hamiltonian. This feature properly distinguishes the FQCs studied in this work from both the purely geometric on-site and the chemically unrealistic transfer models, which have been extensively considered in the physical and mathematical literature during the last three decades.[3, 28–31]

In our treatment we will make use of the transfer matrix formalism in order to translate the quasiperiodic order of atoms and bonds in general FQCs to a sequence of elemental block matrices describing the dynamics of electrons moving through the system. In this way we can exploit a renormalization approach based on the transfer matrices set, which was previously introduced to efficiently study tridiagonal Fibonacci Hamiltonians.[20, 24, 32–34] In so doing, we find out that (i) the zeroth order structure of the energy spectrum in the energy-bond strength phase diagram is entirely determined by the characteristic inflation symmetry of the Fibonacci sequence, and (ii) the hierarchical fragmentation pattern of the spectrum, given by the number and location of the main subbands present in it, is determined by the adopted blocking scheme in the renormalization process. Thus, for a given bond strength value, the progressive fragmentation of the energy spectrum results from resonance effects among certain atomic clusters of progressively increasing size at different scales. Therefore, long-range correlations stemming from the local isomorphism symmetry characteristic of quasiperiodic order ultimately determine the nested hierarchical structure of the energy spectrum in general FQCs. In order to properly describe this hierarchical structure we introduce a suitable algebraic approach allowing for a unified and systematic mathematical description of the spectrum splitting patterns by means of commutators involving a number of basic block matrices related to those atomic clusters. In this way, we obtain closed analytical expressions for the energy spectrum structure in terms of the roots of energy dependent polynomials whose degree is given by successive Fibonacci numbers.

FIBONACCI QUASICRYSTAL ALLOY MODEL

Within the independent electron approximation the electron dynamics through a given one-dimensional lattice can be described in terms of a tight-binding model given by the

Schrödinger equation (in $\hbar = 2m = 1$ units)

$$(E - V_k)\psi_k - t_{k,k-1}\psi_{k-1} - t_{k,k+1}\psi_{k+1} = 0, \tag{1}$$

where E is the electron energy, the on-site energies V_k account for the atomic potentials at the k-th lattice site, the transfer integrals $t_{k,k\pm1}$ measure the hopping amplitudes of the electron between neighbouring atoms, and ψ_k stands for the amplitude of the wave function at site k. In the mathematical literature Eq.(1) is referred to as a substitution Jacobi operator, related to the discrete Hamiltonian

$$(H\psi)_k = a_{k+1}\psi_{k+1} + a_k\psi_{k-1} + b_k\psi_k, \tag{2}$$

where $a_{k+1} \equiv t_{k,k+1}$, $a_k \equiv t_{k,k-1}$, and $b_k \equiv V_k$, so that the discrete Laplacian $a_{k+1}\psi_{k+1} + a_k\psi_{k-1}$ represents the kinetic energy, and $b_k\psi_k$ represents the potential energy.[35]

In this work we will study Eq.(1) by considering one-dimensional binary alloys where two kinds of atoms, say A and B, are arranged according to the Fibonacci sequence, so that the total number of atoms in the lattice is $N = F_j$, where $F_{j+1} = F_j + F_{j-1}$, with $F_0 = F_1 = 1$, is a Fibonacci number. Since the nature of bonds linking different atoms depends on their chemical nature, the quasiperiodic arrangement of atoms naturally induces a quasiperiodic sequence of bonds in our system, whose strength is measured in terms of the transfer integrals $t_{AB} = t_{BA}$ and t_{AA} in Eq.(1). Indeed, the possible existence of two consecutive B atoms is not allowed in a Fibonacci sequence, resulting in the presence of two possible kinds of bonds, namely, $A-A$ and $A-B$ ($B-A$), in a FQC. Accordingly, our FQC model is characterized by the existence of *both* atomic and chemical bonding quasiperiodic distributions.[36] The resulting sequences of atomic potentials $\{V_k\}$ and bonds $\{t_{k,k+1}\}$ is illustrated in Fig. 1(a) for a FQC containing $N = F_6 = 13$ atoms.

In order to disclose the nature of the correlation between both sequences, the lattice shown in Fig. 1(a) is resolved in terms of $A-A$ dimers and $A-B-A$ trimers, respectively labeled β and α in Fig. 1(b), to obtain the sequence of α and β atomic clusters shown in Fig.1(c)-(d). In so doing, overlapping of neighbouring $A-A$ and $A-B-A$ clusters is allowed by sharing their respective ending atoms, as it is highlighted in Fig. 1(b).[37] In this way, we realize that the sequence of bonds in a FQC containing F_j atoms can be grouped in terms of F_{j-1} clusters, which are arranged themselves according to the Fibonacci sequence given by the substitution rule $g(\alpha) = \alpha\beta$ and $g(\beta) = \alpha$ starting with α.

pssb Macia.pdf

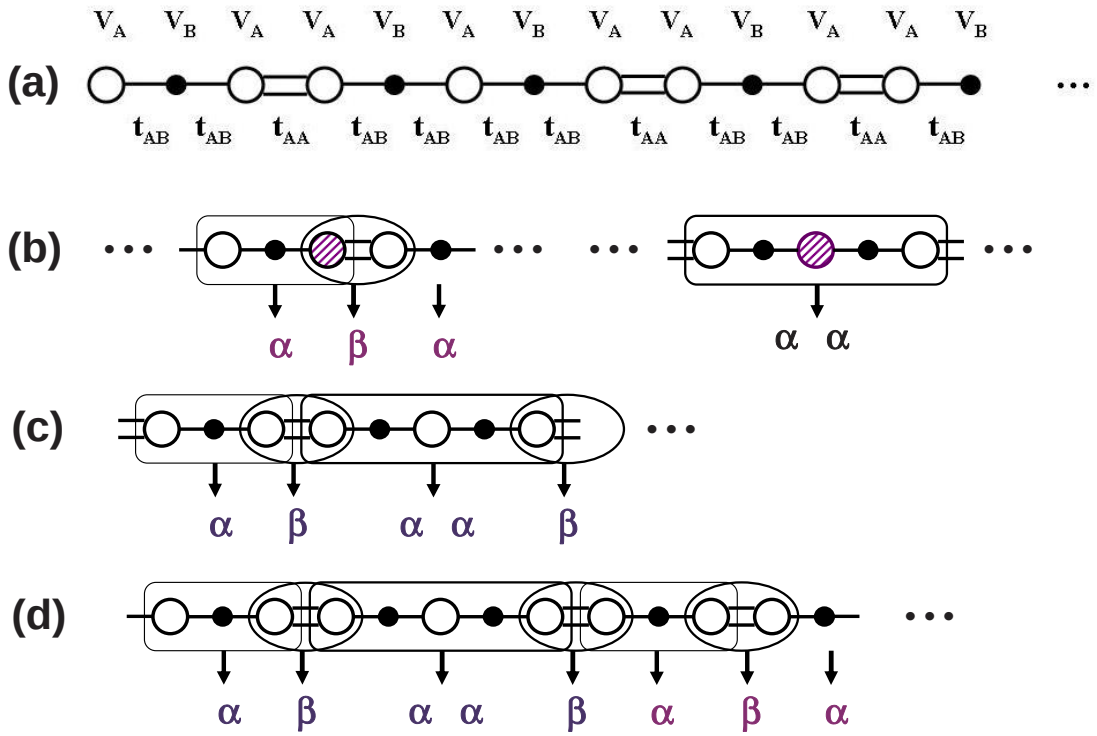

FIG. 1: The structure of the original FQC shown in (a) is resolved in terms of overlapping AA and ABA clusters, respectively labeled β and α, as it is shown in (b), where shared neighboring atoms are dashed. The resulting sequence of atomic clusters α and β is arranged according to the Fibonacci sequence, as it is illustrated in (c) and (d).

The wave function amplitudes in Eq.(1) can be recursively obtained according to the expression

$$\begin{pmatrix} \psi_{N+1} \\ \psi_N \end{pmatrix} = \prod_{k=N}^{1} \mathbf{M}_k \begin{pmatrix} \psi_1 \\ \psi_0 \end{pmatrix} \equiv \mathcal{M}_N(E) \begin{pmatrix} \psi_1 \\ \psi_0 \end{pmatrix}, \tag{3}$$

where

$$\mathbf{M}_k \equiv \mathbf{M}_{k-1,k,k+1} = \begin{pmatrix} \frac{E-V_k}{t_{k,k+1}} & -\frac{t_{k,k-1}}{t_{k,k+1}} \\ 1 & 0 \end{pmatrix}, \tag{4}$$

is referred to as the local transfer matrix, and $\mathcal{M}_N(E)$ is the so-called global transfer matrix. Making use of Eqs.(3) and (4) it has been recently proved,[38] on the basis of the trace map

formalism,[39, 40] that the spectrum of the general tridiagonal Hamiltonian given by Eq.(2) is a Cantor set of zero Lebesgue measure belonging to the purely singular continuous type, thereby extending the results previously rigorously proved for diagonal and off-diagonal models only. Furthermore, the spectrum has a multifractal Hausdorff dimension, instead of a simple fractal single-valued one, which depends on the adopted a_k and b_k values in the general tridiagonal case.[38] Since both the Laplacian and the potential terms in Eq.(2) follow a substitution Fibonacci sequence in general FQCs, the above results are applicable to our proposed model, hence indicating that the inner structure of the energy spectrum of a tridiagonal FQC model is richer than that corresponding to the diagonal and off-diagonal simpler models. In the following section we will disclose the main features of its structure by considering a renormalization method based on the properties of the transfer matrices.

DISCLOSING THE ELECTRONIC SPECTRUM STRUCTURE

The elemental block matrices

According to Eq.(3) the underlying quasiperiodic order of the atoms and bonds in FQCs is naturally encoded in the specific order of appearance of the local transfer matrices in $\mathcal{M}_N(E)$, as well as by the number of different kinds of local transfer matrices which must be considered in the $\mathcal{M}_N$ product. This matrix product can be renormalized by introducing the matrix blocks $\mathbf{r} \equiv \mathbf{M}_{BAB}\mathbf{M}_{ABA}$ and $\mathbf{R} \equiv \mathbf{M}_{AAB}\mathbf{M}_{BAA}\mathbf{M}_{ABA}$, so that the renormalized global transfer matrix reads $\mathcal{M}_N(E) = \ldots\mathbf{RrRrRRrR}$, and it depends on just *two* matrices arranged according to the Fibonacci sequence given by the substitution rule $g(\mathbf{r}) = \mathbf{R}$ and $g(\mathbf{R}) = \mathbf{rR}$.[24, 32] Thus, the quasiperiodic order of the original distribution of atoms and bonds in the FQC is preserved in the renormalized matrix sequence describing its electron dynamics. It can be shown by induction that this matrix sequence contains $n_R = F_{j-3}$ matrices $\mathbf{R}$ and $n_r = F_{j-4}$ matrices $\mathbf{r}$, where $F_j = N$ is the number of atoms in the FQC. Thereafter, we will refer to $\mathbf{r}$ and $\mathbf{R}$ as the *elemental block* matrices.

From a physical point of view these matrices respectively describe the electron dynamics through the *minimal* atomic clusters BA and BAA in terms of which the entire FQC can be decomposed via an exact deflation process.[41, 42] Making use of Eq.(4) their traces can be written $\mathrm{tr}(\mathbf{r}) = E^2 - a^2 \equiv p_2(E)$, with $a^2 \equiv \epsilon^2 + 2$, and $\mathrm{tr}(\mathbf{R}) = \gamma^{-1}p_3(E)$, with

$p_3(E) \equiv E^3 - \epsilon E^2 - (\gamma^2 + a^2)\, E - \epsilon\,(\gamma^2 - a^2)$, where the subscripts denote the polynomial degree, and where the origin of energies is defined in such a way that $V_A = -V_B \equiv \epsilon$, $\gamma \equiv t_{AA}/t_{AB}$, and the energy scale is given by $t_{AB} \equiv 1$ without loss of generality. As we see, these trace related polynomials depend on both the on-site energies and the $A - A$ relative bond strength through the model parameters ϵ and γ, respectively. Making use of these polynomials the elemental block matrices can be written

$$\mathbf{r} = \begin{pmatrix} p_2 + 1 & \epsilon - E \\ \epsilon + E & -1 \end{pmatrix}, \;\; \mathbf{R} = \gamma^{-1} \begin{pmatrix} p_3 + E - \epsilon & \gamma^2 - (E - \epsilon)^2 \\ p_2 + 1 & \epsilon - E \end{pmatrix}. \tag{5}$$

As it can be readily checked $\det \mathbf{r} = \det \mathbf{R} = 1$, so that $\mathcal{M}_N(E) \in SL(2, \mathbb{R})$ group.

Inflation symmetry related commutators

In order to analyze the role of the characteristic scale-invariance symmetry in the energy spectrum structure of FQCs, we will consider commutators containing progressively longer string products of elemental blocks matrices $\mathbf{r}$ and $\mathbf{R}$, as prescribed by the successive application of the Fibonacci substitution rule. These Fibonacci matrix strings can be recursively obtained from the concatenation formula $\mathbf{F}_n = \mathbf{F}_{n-1}\mathbf{F}_{n-2}$, $n \geq 2$, starting with $\mathbf{F}_0 \equiv \mathbf{r}$, $\mathbf{F}_1 \equiv \mathbf{R}$.[43] Therefore, the resulting matrix blocks express the characteristic inflation symmetry of FQCs in a natural way, and we will refer to them as *Fibonacci blocks*. Since $\det \mathbf{r} = \det \mathbf{R} = 1$, all Fibonacci blocks belong to the $SL(2, \mathbb{R})$ group. The first members of the commutator series we are interested in read

$$g[\mathbf{R}, \mathbf{r}] \equiv [g(\mathbf{R}), g(\mathbf{r})] = [\mathbf{R}\mathbf{r}, \mathbf{R}] = -\mathbf{R}[\mathbf{R}, \mathbf{r}]. \tag{6}$$

To obtain the next members in a systematic way we will exploit the concatenation property of Fibonacci blocks $\mathbf{F}_n$, so that any commutator involving two successive arbitrary blocks can be expressed in the form

$$g^n[\mathbf{R}, \mathbf{r}] \equiv [\mathbf{F}_{n+1}, \mathbf{F}_n] = \mathbf{F}_n\mathbf{F}_{n-1}\mathbf{F}_n - \mathbf{F}_n\mathbf{F}_n\mathbf{F}_{n-1} = -\mathbf{F}_n[\mathbf{F}_n, \mathbf{F}_{n-1}], \tag{7}$$

where $n \geq 1$ indicates the inflation stage. The expressions above can be recursively iterated to obtain

$$g^n[\mathbf{R}, \mathbf{r}] = (-1)^n \prod_{j=n}^{1} \mathbf{F}_j \; [\mathbf{R}, \mathbf{r}] \equiv (-1)^n \; \mathbf{\Phi}_n \; [\mathbf{R}, \mathbf{r}]. \tag{8}$$

Therefore, commutators including progressively longer Fibonacci blocks can be expressed in terms of the *elemental commutator* $[\mathbf{R}, \mathbf{r}]$, along with a string product of Fibonacci blocks given by $\mathbf{\Phi}_n$. Making use of (5) we obtain,

$$[\mathbf{R}, \mathbf{r}] = \gamma^{-1} p_1 \begin{pmatrix} 1 & 0 \\ \epsilon + E & -1 \end{pmatrix} \equiv \gamma^{-1} p_1 \mathbf{F}, \tag{9}$$

where

$$p_1(E) = \left(\gamma^2 - 1\right) E + \epsilon \left(\gamma^2 + 1\right). \tag{10}$$

We note that, in the case $\gamma = 1$, which corresponds to the on-site diagonal model, this polynomial reduces to the constant value $p_1 = 2\epsilon$, so that there do not exist resonance energies for this model, as it is well known.[44] We also note that $\mathbf{F}$ has null trace and $\det \mathbf{F} = -1$, so that, although both $\mathbf{R}$ and $\mathbf{r}$ belong to the $SL(2, \mathbb{R})$ group, the commutator $[\mathbf{R}, \mathbf{r}]$ does not.[45] The $\mathbf{F}$ matrix satisfies the relationships $\mathbf{F}^2 = \mathbf{I}$, where $\mathbf{I}$ is the 2×2 identity matrix, and

$$\mathbf{rFr} = \mathbf{F}, \quad \mathbf{RFR} = \mathbf{F}. \tag{11}$$

By plugging Eq.(9) in Eq.(8) one has

$$g^n[\mathbf{R}, \mathbf{r}] = (-1)^n \gamma^{-1} p_1 \ \mathbf{\Phi}_n \mathbf{F}. \tag{12}$$

Thus, in order to look for the possible existence of resonance energies satisfying the condition $g^n[\mathbf{R}, \mathbf{r}] = \mathbf{0}$ (alternatively, $\tilde{g}^n[\mathbf{R}, \mathbf{r}] = \mathbf{0}$) for any $n \geq 1$, one must consider the algebraic equation $p_1(E) = 0$, along with the matrix equation $\mathbf{\Phi}_n \mathbf{F} = \mathbf{0}$ (alternatively, $\mathbf{F}\tilde{\mathbf{\Phi}}_n = \mathbf{0}$). Now, we know that $\mathbf{F} \neq 0$ and $\det \mathbf{F} \neq 0$ for any energy value. On the other hand, since $\mathbf{F}_n \in SL(2, \mathbb{R})\ \forall n$, the string products $\mathbf{\Phi}_n$ and $\tilde{\mathbf{\Phi}}_n$ are themselves unimodular, so that $\det \mathbf{\Phi}_n = \det \tilde{\mathbf{\Phi}}_n = 1$. Therefore, since the necessary condition for the equation $\mathbf{M}_1 \mathbf{M}_2 = \mathbf{0}$ to be satisfied by two arbitrary square matrices ($\mathbf{M}_1 \neq \mathbf{0}$ and $\mathbf{M}_2 \neq \mathbf{0}$) is that one of the matrices appearing in the product has zero determinant, we conclude that $\mathbf{\Phi}_n \mathbf{F} \neq \mathbf{0}$ and $\mathbf{F}\tilde{\mathbf{\Phi}}_n \neq \mathbf{0}$, $\forall n \geq 1$.

Consequently, at any arbitrary inflation stage the commutation condition $g^n[\mathbf{R}, \mathbf{r}] = \mathbf{0}$ (alternatively, $\tilde{g}^n[\mathbf{R}, \mathbf{r}] = \mathbf{0}$) reduces to the algebraic equation $p_1(E) = 0$, leading to the *same* resonance energy

$$E_* = \epsilon \, \frac{1 + \gamma^2}{1 - \gamma^2}, \quad \forall n. \tag{13}$$

This energy depends on the model parameters ϵ and $\gamma \neq 1$ ($\gamma = 1$ has no physical meaning in a FQC), i.e., $E_*(\gamma, \epsilon)$. The parametric curve $E_*(\gamma, \epsilon)$ thus defines the zeroth order energy spectrum structure for any FQC. This curve is even with respect to γ (i.e., $E_*(-\gamma, \epsilon) = E_*(\gamma, \epsilon)$) and odd with respect to ϵ (i.e., $E_*(\gamma, -\epsilon) = -E_*(\gamma, \epsilon)$). It also exhibits the bonding exchange symmetry $E_*(\gamma^{-1}, \epsilon) = -E_*(\gamma, \epsilon)$, $\forall \gamma \neq 1$, under permutation of the bond strength values between $A - A$ and $A - B$ pairs. For a given γ value, E_* scales linearly with ϵ, whereas for a given ϵ value E_* varies with γ in a significant non-linear way, and displays vertical asymptotes in the limits $\gamma = \pm 1$. Since E_* is the only solution to the resonance conditions $g^n[\mathbf{R}, \mathbf{r}] = \mathbf{0}$, for any $n \geq 1$, the resonance energy value given by Eq.(13) becomes extremely degenerate as one considers commutators involving progressively longer Fibonacci blocks, approaching the quasiperiodic limit $n \to \infty$. Therefore, the global scale inflation symmetry, described in terms of the successive application of the characteristic Fibonacci substitution rule g, *does not* account for the progressive fragmentation of the energy spectrum by its own.

Local isomorphism related commutators

Let us now consider multi-scale, long-range correlations described by means of commutators involving *non-successive* generation Fibonacci blocks of the form $[\mathbf{F}_{n+k}, \mathbf{F}_n]$ (alternatively, $[\tilde{\mathbf{F}}_{n+k}, \tilde{\mathbf{F}}_n]$), with $k \geq 2$. Let us start by considering the case $k = 2$. Taking into account the concatenation property of Fibonacci blocks and making use of Eqs.(8) and (9) we have

$$[\mathbf{F}_{n+2}, \mathbf{F}_n] = [\mathbf{F}_{n+1}, \mathbf{F}_n]\mathbf{F}_n = (-1)^n \gamma^{-1} p_1 \mathbf{\Phi}'_n \mathbf{F}_n, \tag{14}$$

where $\mathbf{\Phi}'_n \equiv \mathbf{\Phi}_n \mathbf{F}$, with $n \geq 1$. The obtained expressions are formally equivalent to those given by Eq.(12), and since $\det \mathbf{\Phi}'_n = -1$ and the Fibonacci block matrices are unimodular, the resonance conditions $[\mathbf{F}_{n+2}, \mathbf{F}_n] = \mathbf{0}$ reduce to the well-known equation $p_1(E) = 0$ leading to Eq.(13). On the contrary, for the case $k = 3$ we get

$$[\mathbf{F}_{n+3}, \mathbf{F}_n] = [\mathbf{F}_{n+1}\mathbf{F}_n\mathbf{F}_{n+1}, \mathbf{F}_n] = (-1)^n \gamma^{-1} p_1 \mathrm{tr}\mathbf{F}_{n+2}\ \mathbf{\Phi}_n \mathbf{F}, \tag{15}$$

with $n \geq 1$, where we have used Eqs.(8) and (9) along with Eq.(46) given in the Appendix. By comparing with Eq.(12), which gives the commutators corresponding to two arbitrary but *consecutive* Fibonacci blocks, we see that Eq.(15) differs by the presence of the factor $\mathrm{tr}\mathbf{F}_{n+2}$.

In order to gain a deeper insight on the important physical role played by the presence of this factor, it is convenient to introduce a family of polynomials which are related to the traces of the Fibonacci blocks. Indeed, since $\mathbf{F}_n$ matrices are unimodular and they obey the concatenation rule $\mathbf{F}_{n+1} = \mathbf{F}_n\mathbf{F}_{n-1}$, their traces satisfy the recursion relation,[39, 46]

$$\mathrm{tr}\mathbf{F}_{n+1} = \mathrm{tr}\mathbf{F}_n\mathrm{tr}\mathbf{F}_{n-1} - \mathrm{tr}\mathbf{F}_{n-2}, \quad n \geq 2, \tag{16}$$

with $\mathrm{tr}\mathbf{F}_0 \equiv \mathrm{tr}(\mathbf{r}) = p_2$, $\mathrm{tr}\mathbf{F}_1 \equiv \mathrm{tr}(\mathbf{R}) = \gamma^{-1}p_3$, and $\mathrm{tr}\mathbf{F}_2 \equiv \mathrm{tr}(\mathbf{Rr}) = \mathrm{tr}(\mathbf{rR}) = \gamma^{-1}p_5$, where $p_5(E) \equiv p_2p_3 - E + \epsilon$, is obtained from Eq.(5) by explicit multiplication. Making use of Eq.(16) recursively we obtain

$$\mathrm{tr}\mathbf{F}_3 = \mathrm{tr}\mathbf{F}_2\mathrm{tr}\mathbf{F}_1 - \mathrm{tr}\mathbf{F}_0 = \gamma^{-2}p_5p_3 - p_2 \equiv \gamma^{-2}p_8, \tag{17}$$

$$\mathrm{tr}\mathbf{F}_4 = \mathrm{tr}\mathbf{F}_3\mathrm{tr}\mathbf{F}_2 - \mathrm{tr}\mathbf{F}_1 = \gamma^{-3}p_8p_5 - \gamma^{-1}p_3 \equiv \gamma^{-3}p_{13}, \tag{18}$$

$$\mathrm{tr}\mathbf{F}_5 = \mathrm{tr}\mathbf{F}_4\mathrm{tr}\mathbf{F}_3 - \mathrm{tr}\mathbf{F}_2 = \gamma^{-5}p_{13}p_8 - \gamma^{-1}p_5 \equiv \gamma^{-5}p_{21}, \tag{19}$$

$$\ldots$$

$$\mathrm{tr}\mathbf{F}_j = \mathrm{tr}\mathbf{F}_{j-1}\mathrm{tr}\mathbf{F}_{j-2} - \mathrm{tr}\mathbf{F}_{j-3} = \gamma^{-F_{j-1}}p_{F_{j+2}}, \quad j \geq 3, \tag{20}$$

where we have defined the energy dependent polynomials

$$p_{F_j}(E) \equiv p_{F_{j-1}}p_{F_{j-2}} - \gamma^{2F_{j-5}}p_{F_{j-3}}, \quad j \geq 5, \tag{21}$$

whose degree is given by Fibonacci numbers. Henceforth, we will refer to the polynomials introduced in Eq.(21) as *Fibonacci spectral polynomials*.[47]

By plugging Eqs.(20) and (21) into Eq.(15) we obtain

$$[\mathbf{F}_{n+3}, \mathbf{F}_n] = (-1)^n\gamma^{-(1+F_{n+1})}p_1p_{F_{n+4}}\ \mathbf{\Phi}_n\mathbf{F}, \tag{22}$$

with $n \geq 1$. Therefore, when one considers commutators involving non-consecutive Fibonacci blocks of the form $\mathbf{F}_{n+k}$, satisfying the threshold condition $k \geq 3$, the resonance conditions $[\mathbf{F}_{n+3}, \mathbf{F}_n] = \mathbf{0}$ naturally lead to new energy levels given by the roots of the Fibonacci spectral polynomials $p_{F_{n+4}}(E) = 0$, with $n \geq 1$. Physically this means that for a given atomic cluster, corresponding to the Fibonacci block F_n, resonant effects involving atomic clusters related to the next and second-next Fibonacci blocks F_{n+1} and F_{n+2} are ineffective in order to give rise to novel energy levels in the energy spectrum. To this end, at least third generation related Fibonacci blocks are required, thereby indicating the existence of a generation threshold value for the emergence of hierarchical nested structure in the spectra of FQCs.

pssb Macia.pdf

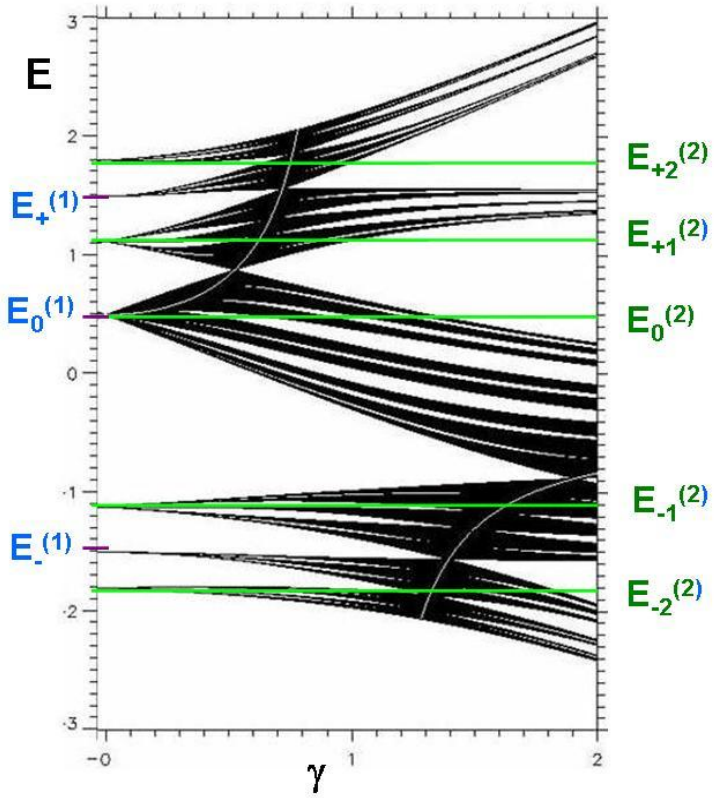

FIG. 2: Numerically obtained phase diagram for a FQC with $N = 34$ atoms and on-site energy $\epsilon = 1/2$, over the range $0 \leq \gamma \leq 2$. The zeroth-order energy spectrum given by Eq.(13) is highlighted with a thin white line. The regions closer to this line are densely populated as a consequence of the high degeneration of the resonance energy E_*. The ABA molecule energy levels corresponding to the weak coupling limit, $E_0^{(1)} = 1/2$ and $E_\pm^{(1)} = \pm 3/2$, are indicated in the ordinate axis on the left. On the right, we indicate the energy values of the pentamer $ABABA$ molecule, $E_0^{(2)} = 1/2$, $E_{\pm 1}^{(2)} = \pm\sqrt{5}/2$, and $E_{\pm 2}^{(2)} = \pm\sqrt{13}/2$ (horizontal green lines).

Weak $A-A$ bonding energy spectrum

Very interesting results regarding the energy spectrum structure of FQCs can be obtained in terms of the Fibonacci spectral polynomials. In fact, in the case $\gamma = 0$ Eq.(21) adopts the factorized form $p_{F_j} = p_{F_{j-1}} p_{F_{j-2}}$ ($j \geq 5$), with $p_2 = E^2 - a^2$, $p_3 = (E - \epsilon)p_2$, and

$p_5 = (E-\epsilon)(p_2^2-1)$, so that by induction one readily obtains the general expression

$$p_{F_j}(E) = (E-\epsilon)^{F_{j-3}}(p_2^2-1)^{F_{j-4}}p_2^{F_{j-5}},\ j \geq 5, \tag{23}$$

whose roots are given by $E=\epsilon$, $p_2 = 0 \Longrightarrow E_{\pm}^{(1)} = \pm\sqrt{\epsilon^2+2}$, and $p_2 = \pm 1 \Longrightarrow E = \epsilon$, $E_{\pm 1}^{(2)} = \pm\sqrt{\epsilon^2+1}$, and $E_{\pm 2}^{(2)} = \pm\sqrt{\epsilon^2+3}$.[48] *For the sake of illustration, in Fig.2 the location of these resonance energies is indicated in a numerically obtained phase diagram for a FQC with* $N = 34$ *atoms and* $\epsilon = 1/2$.

A close inspection to the phase diagram shown in Fig. 2 clearly shows that the overall energy spectrum becomes progressively simpler and its fragmentation degree significantly reduces as one approaches the limit $\gamma \to 0$. Physically this limit describes a systematic weakening of bonds between the atoms composing the $A-A$ dimers, which effectively break apart when the antibonding condition $t_{AA} = 0$ is attained. In that case the original FQC fragments itself into a series of ABA trimers and $ABABA$ pentamers (see Fig.1(a)). Their corresponding molecular energy levels are $E_0^T = \epsilon$ and $E_{\pm}^T = \pm\sqrt{\epsilon^2+2}$, for the trimers, and $E_0^P = \epsilon$, $E_{\pm 1}^P = \pm\sqrt{\epsilon^2+1}$, and $E_{\pm 2}^P = \pm\sqrt{\epsilon^2+3}$, for the pentamers. As we see, these clusters' energy level exactly coincide with the Fibonacci spectral polynomials roots previously obtained, where the energy levels $E_0^T = E_0^P = \epsilon$ are degenerate, their common value coinciding with the zeroth order resonance energy $E_*(\epsilon, 0)$. The energy spectrum structure of a FQC in the weak $A-A$ bonding limit can then be understood as stemming from resonance effects involving the molecular energy levels corresponding to the ABA and $ABABA$ clusters alone, which explains the relatively simpler fragmentation structure of the energy spectrum for small γ values, consisting of seven main bands, as it is illustrated in Fig.2. As the coupling between $A-A$ atoms increases, the onset of *multiple* resonant effects among progressively longer atomic clusters at different scales will split these degenerate molecular levels, giving rise to a gradual fragmentation of the energy spectrum.

HIERARCHICAL STRUCTURE OF THE ENERGY SPECTRUM

To this end, we must consider alternative blocking schemes, involving progressively longer atomic clusters at different scales. In order to proceed in a systematic way, we will begin by considering blocking schemes involving the elemental matrices **R** and **r**, along with their related doublets **Rr**, **rR**, and **RR** (note that **rr** pairs are forbidden by construction in

FQCs). Afterwards, we will study ensembles consisting of increasingly longer blocks. As the considered scale length linearly increases with the block size itself this approach allows us to study the emergence of long-range quasiperiodic order fingerprints in the resulting energy spectrum as we approach the asymptotic $N \to \infty$ and $n \to \infty$ limits in a natural way.

First order fragmentation pattern

Let us consider the FQC renormalized global transfer matrix $\mathcal{M}_N = \ldots \mathbf{RrRRrRrRRrRRrRrRRrRrR}$. There exist six blocking schemes in which this matrix string can be grouped in terms of single and double elemental matrices blocks. Two of them, namely, $\ldots(\mathbf{Rr})\mathbf{R}(\mathbf{Rr})(\mathbf{Rr})\mathbf{R}(\mathbf{Rr})\mathbf{R}(\mathbf{Rr})$, and $\ldots \mathbf{R}(\mathbf{rR})\mathbf{R}(\mathbf{rR})(\mathbf{rR})\mathbf{R}(\mathbf{rR})\mathbf{R}(\mathbf{rR})$, are respectively related to the commutators $[\mathbf{Rr}, \mathbf{R}] = g[\mathbf{R}, \mathbf{r}]$ and $[\mathbf{rR}, \mathbf{R}] = \tilde{g}[\mathbf{R}, \mathbf{r}]$, which were considered in the previous Section (where we saw they only contribute to the resonance energy E_* belonging to the zeroth order energy spectrum). The remaining blocking schemes include $\mathbf{RR}$ pair blocks, and the related commutators are respectively given by $[\mathbf{RR}, \mathbf{r}]$, $[\mathbf{RR}, \mathbf{Rr}]$, and $[\mathbf{RR}, \mathbf{rR}]$, along with $[\mathbf{RR}, \mathbf{R}]$, which trivially vanishes. The non-trivial commutators above can be easily evaluated by expressing the $\mathbf{RR}$ product in the power form

$$\mathbf{R}^2 = (\mathrm{tr}\mathbf{F}_1)\mathbf{R} - \mathbf{I} = \gamma^{-1} p_3 \mathbf{R} - \mathbf{I}, \tag{24}$$

where we made use of Eq.(42) given in the Appendix. Accordingly, the commutators we are interested in read

$$[\mathbf{RR}, \mathbf{r}] = \gamma^{-2} p_1 p_3 \mathbf{F}, \quad [\mathbf{RR}, \mathbf{Rr}] = \gamma^{-2} p_1 p_3 \mathbf{RF}, \quad [\mathbf{RR}, \mathbf{rR}] = \gamma^{-2} p_1 p_3 \mathbf{FR}, \tag{25}$$

where we have used Eqs.(24), (9) and (6). Now, we know that $\mathbf{F} \neq \mathbf{0}$, $\mathbf{RF} \neq \mathbf{0}$ and $\mathbf{FR} \neq \mathbf{0}$ $\forall E$, so that the resonance condition for the commutators (25) requires that $p_1(E) = 0$ and/or $p_3(E) = 0$. Therefore, in addition to the resonance energy E_* given by Eq.(13), we have three *new* resonance energy values given by the roots of the Fibonacci spectral polynomial $p_3(E)$, which define the first order hierarchy of the energy spectrum fragmentation pattern. We note that the simultaneous presence of the polynomials p_1 and p_3 in the factorized Eq.(25) naturally accounts for the overall *nested* structure of the resulting spectrum.

pssb Macia.pdf

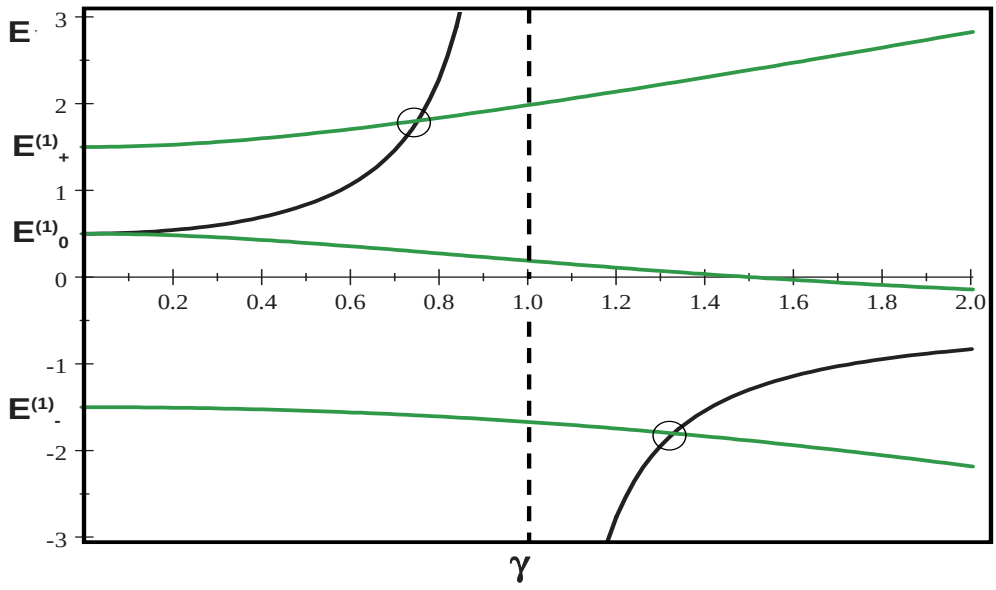

FIG. 3: Analytical phase diagram for a FQC with $\epsilon = 1/2$, over the $A-A$ bond strength range $0 \leq \gamma \leq 2$, showing the zeroth order (in black) and the first order (in green) energy spectrum fragmentation pattern contributions. In the weak coupling limit $\gamma \to 0$ the spectrum consists of three bands located at the ABA molecule energy levels $E_0^{(1)} = 1/2$ and $E_\pm^{(1)} = \pm 3/2$. As soon as the $A-A$ atomic coupling becomes non-negligible the spectrum consists of four bands due to the splitting of the degenerate $E_0^T = E_*$ level, except for those γ values satisfying the band crossing condition $p_3(E_*, \epsilon, \gamma) = 0$ (encircled points). The crossing points exact coordinates in the phase diagram are $(\frac{\sqrt{3}}{6}\left(\sqrt{13}-1\right), \frac{\sqrt{13}}{2})$ and $(\frac{\sqrt{3}}{6}\left(\sqrt{13}+1\right), -\frac{\sqrt{13}}{2})$. We note that the ordinate values of the encircled crossing points coincide with the energy values of the second order fragmentation energies $E_{\pm 2}^{(2)}$ in the weak coupling limit (see Fig.2).

For the sake of illustration the first order energy spectrum, determined by the parametric curves $p_1(E, \epsilon, \gamma) = 0$ and $p_3(E, \epsilon, \gamma) = 0$, is plotted in Fig. 3 for a FQC composed of atoms with on-site energies $V_A = 1/2 = -V_B$, within the $A-A$ bond strength range $0 \leq \gamma \leq 2$. As we see, the total number of bands present in the energy spectrum depends on the adopted γ value. In the weak coupling limit we have $p_3(E, \epsilon, 0) = E^3 - \epsilon E^2 - a^2 E + a$

$^2\epsilon$, whose roots $E_0^{(1)} = \epsilon$, $E_\pm^{(1)} = \pm\sqrt{\epsilon^2+2}$, coincide with the energy levels of the ABA molecule, so that the resulting energy spectrum only displays three main bands. As the $A-A$ atomic coupling increases the doubly degenerated level $E_0^{(1)} = \epsilon = E_0^{(0)}$, splits and the energy spectrum consists of four bands instead, except for those γ values satisfying the condition $E_*(\epsilon,\gamma) = E_\pm^{(1)}(\epsilon,\gamma)$, leading to double degenerate states in the upper and lower bands, thereby rendering a trifurcated spectrum as well. The corresponding crossing points (encircled in Fig. 3) can be analytically obtained from the condition $p_3(E_*,\epsilon,\gamma) = 0$, to get $\gamma_\pm = \sqrt{b \pm \sqrt{b^2-1}}$, with $b \equiv 1 + 2\epsilon^2/3$. Finally, we note that $\lim_{\gamma\to\infty} E_*(\epsilon,\gamma) = \lim_{\gamma\to\infty} E_0^{(1)}(\epsilon,\gamma) = -\epsilon$, which also leads to a nearly trifurcation pattern of the energy spectrum in the very strong $A-A$ bonding regime.

Second order fragmentation pattern

In order to describe the next hierarchy level in the energy spectrum structure we will consider blocking schemes including suitable triplets of elemental clusters matrices $\mathbf{r}$ and $\mathbf{R}$. To this end, we recall that the blocking scheme consisting of the Fibonacci blocks $\mathbf{RrR} = \mathbf{F}_3$ and $\mathbf{R} = \mathbf{F}_1$ do not contribute to the fragmentation of the energy spectrum. Thus, we have identified three possible blocking schemes, namely: (1) $\mathbf{RrR}$ triplets along with single $\mathbf{r}$ matrices, (2) $\mathbf{rRr}$ triplets along with single $\mathbf{R}$ matrices, and (3) $\mathbf{rRr}$ triplets along with $\mathbf{RR}$ pairs. The corresponding commutators read,

$$[\mathbf{RrR},\mathbf{r}] = \mathrm{tr}\mathbf{F}_2[\mathbf{R},\mathbf{r}] = \gamma^{-2}p_1p_5\mathbf{F}, \quad [\mathbf{rRr},\mathbf{R}] = -\mathrm{tr}\mathbf{F}_2[\mathbf{R},\mathbf{r}] = -\gamma^{-2}p_1p_5\mathbf{F}, \tag{26}$$

$$[\mathbf{rRr},\mathbf{RR}] = [\mathbf{rRr},(\mathrm{tr}\mathbf{F}_1)\mathbf{R}-\mathbf{I}] = \mathrm{tr}\mathbf{F}_1[\mathbf{rRr},\mathbf{R}] = -\gamma^{-3}p_1p_3p_5\mathbf{F}, \tag{27}$$

where we have used Eq.(46) given in the Appendix along with Eqs.(9), (24), and (26), respectively. It is worth noticing that the commutators involving the blocks $\mathbf{rRr}$ and $\mathbf{RrR}$ in Eq.(26) are mutually related through the *conjugation* operation $\mathcal{C} : \mathbf{r} \longleftrightarrow \mathbf{R}$, so that one gets the relationship $\mathcal{C}[\mathbf{RrR},\mathbf{r}] = -[\mathbf{rRr},\mathbf{R}]$.

By comparing Eqs.(26) and (27) we see that the Fibonacci spectral polynomial p_3 appears in the factorized expression of commutator $[\mathbf{rRr},\mathbf{RR}]$, but it does not appear in the expressions of both commutators $[\mathbf{RrR},\mathbf{r}]$ and $[\mathbf{rRr},\mathbf{R}]$. This is due to the fact that the

pssb Macia.pdf

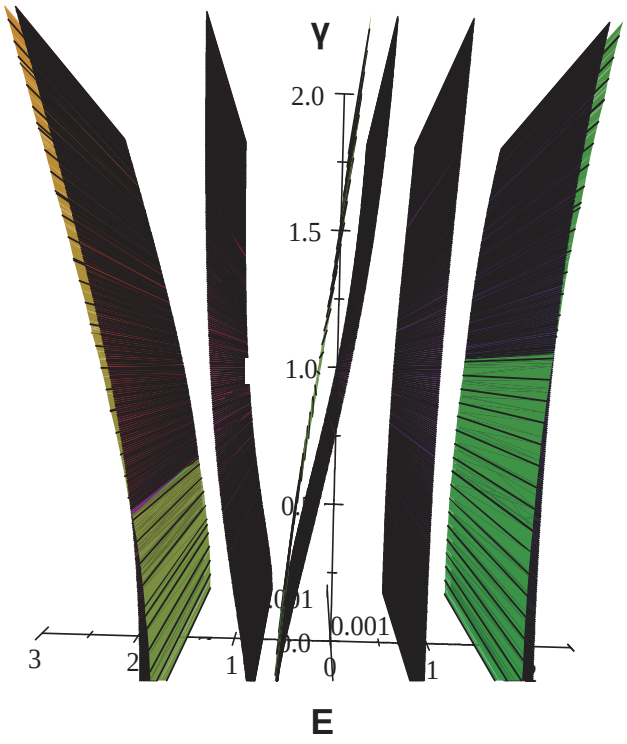

FIG. 4: Second order energy spectrum structure determined by the roots of the Fibonacci spectral polynomial $p_3(E,\epsilon,\gamma)$ and $p_5(E,\epsilon,\gamma)$ for a FQC with $N = 34$ atoms, $\epsilon = 1/2$ and $0 \leq \gamma \leq 3$. The upper and lower bands resolve into two bands belonging to different spectral polynomials each.

effective scale related to these conjugate commutators is shorter than that corresponding to the former one. The presence of the Fibonacci spectral polynomial $p_5(E)$ in the commutators above discloses a new set of resonance energy values, given by the condition $p_5(E) = 0$, which defines the second order fragmentation pattern in the energy spectrum. In the weak bonding limit $\gamma \to 0$ the roots of the polynomial $p_5(E,\epsilon,0) = (E-\epsilon)(p_2^2 - 1)$ coincide with the $ABABA$ molecule energy levels, namely, $E_0^{(2)} = \epsilon$ (note that the energy level $\epsilon = E_0^{(2)} = E_0^{(1)} = E_0^{(0)}$ becomes triply degenerate at this stage of the energy spectrum generation), $E_{\pm 1}^{(2)} = \pm\sqrt{\epsilon^2+1}$, and $E_{\pm 2}^{(2)} = \pm\sqrt{\epsilon^2+3}$, as it is shown in Fig. 2. In Fig. 4 we show the overall structure of the second order hierarchy in the energy spectrum of a

FQC with on-site energy $\epsilon = 1/2$ over the range $0 \leq \gamma \leq 2$.

Third, fourth and fifth order fragmentation patterns

The next hierarchies in the energy spectrum fragmentation pattern are obtained by considering blocking schemes based on the quadruplet block **rRRr** in combination with: (1) isolated **R** matrices, (2) **RR** pairs, and (3) **RrR** triplets. Accordingly, we must consider the following commutators:

$$[\mathbf{rRRr}, \mathbf{R}] = [\mathbf{r}((\mathrm{tr}\mathbf{F}_1)\mathbf{R} - \mathbf{I})\mathbf{r}, \mathbf{R}] = \mathrm{tr}\mathbf{F}_1[\mathbf{rRr}, \mathbf{R}] - [\mathbf{r}^2, \mathbf{R}] \tag{28}$$

$$= -\mathrm{tr}\mathbf{F}_1\mathrm{tr}\mathbf{F}_2[\mathbf{R}, \mathbf{r}] + \mathrm{tr}\mathbf{F}_0[\mathbf{R}, \mathbf{r}] = -\mathrm{tr}\mathbf{F}_3[\mathbf{R}, \mathbf{r}] = -\gamma^{-3}p_1p_8\mathbf{F}, \tag{29}$$

where we have taken into account Eqs.(24), (26), (17), (9), respectively, and we used Eq.(42) to express $\mathbf{r}^2 = (\mathrm{tr}\mathbf{F}_0)\mathbf{r} - \mathbf{I}$.

$$[\mathbf{rRRr}, \mathbf{RR}] = -\mathrm{tr}(\mathbf{RrR})[\mathbf{RR}, \mathbf{r}] = -\mathrm{tr}\mathbf{F}_3\mathrm{tr}\mathbf{F}_1[\mathbf{R}, \mathbf{r}] = -\gamma^{-4}p_1p_3p_8\mathbf{F}, \tag{30}$$

where we made use of (46) and the cyclic permutation property of the trace $\mathrm{tr}(\mathbf{rRR}) = \mathrm{tr}(\mathbf{RrR}) = \mathrm{tr}\mathbf{F}_3$, along with Eqs.(17) and (25).

$$\begin{aligned}[\mathbf{rRRr}, \mathbf{RrR}] &= [\mathbf{r}((\mathrm{tr}\mathbf{F}_1)\mathbf{R} - \mathbf{I})\mathbf{r}, \mathbf{RrR}] = \mathrm{tr}\mathbf{F}_1[\mathbf{rRr}, \mathbf{RrR}] + \mathrm{tr}\mathbf{F}_0[\mathbf{RrR}, \mathbf{r}] \\ &= (\mathrm{tr}\mathbf{F}_1 - \mathrm{tr}\mathbf{F}_2(\mathrm{tr}\mathbf{F}_2\mathrm{tr}\mathbf{F}_1 - \mathrm{tr}\mathbf{F}_0))[\mathbf{R}, \mathbf{r}] = (\mathrm{tr}\mathbf{F}_1 - \mathrm{tr}\mathbf{F}_2\mathrm{tr}\mathbf{F}_3)[\mathbf{R}, \mathbf{r}] \\ &= -\mathrm{tr}\mathbf{F}_4[\mathbf{R}, \mathbf{r}] = -\gamma^{-4}p_1p_{13}\mathbf{F}, \end{aligned} \tag{31}$$

where we have used Eqs.(24), (26), (17) and (18), along with Eqs.(42) and (44) in the Appendix to express,

$$[\mathbf{rRr}, \mathbf{RrR}] \equiv (\mathbf{rR})^3 - (\mathbf{Rr})^3 = (1 - \mathrm{tr}^2\mathbf{F}_2)[\mathbf{R}, \mathbf{r}]. \tag{32}$$

The roots of the Fibonacci spectral polynomials $p_8(E)$ in (29) and (30), and $p_{13}(E)$ in (31), respectively determine the main features of the third and fourth order fragmentation patterns of the energy spectrum.

The fourth order fragmentation pattern can also be obtained by considering blocking schemes including longer blocks, hence involving multiple resonances among different shorter atomic clusters at the considered scale length. For instance, let us consider the commutator

$$[\mathbf{RRrRrRR},\mathbf{rRr}] = -\mathrm{tr}(\mathbf{rRrRR})[\mathbf{rRr},\mathbf{RR}] = -\mathrm{tr}(\mathbf{RrRRr})[\mathbf{rRr},\mathbf{RR}]$$
$$= \mathrm{tr}\mathbf{F}_1\mathrm{tr}\mathbf{F}_2\mathrm{tr}\mathbf{F}_4[\mathbf{R},\mathbf{r}] = \gamma^{-6}p_1p_3p_5p_{13}\mathbf{F}, \tag{33}$$

where we used Eq.(46) taking $\mathbf{A} = \mathbf{rRr}$ and $\mathbf{B} = \mathbf{RR}$, along with Eqs.(27), (26) and (18). As we see, three consecutive fragmentation pattern hierarchies are included via the Fibonacci spectral polynomials p_3, p_5 and p_{13} appearing in the factorized expression of this commutator.

Finally, blocking schemes yielding the fifth order fragmentation pattern involve blocks containing seven elemental block matrices $\mathbf{r}$ and $\mathbf{R}$ at least. The simpler commutator representative is given by,

$$[\mathbf{rRRrRRr},\mathbf{RrR}] = [(\mathbf{rR}^2)^2\mathbf{r},\mathbf{RrR}] = \mathrm{tr}\mathbf{F}_3[\mathbf{rRRr},\mathbf{RrR}] + [\mathbf{RrR},\mathbf{r}]$$
$$= (\ \mathrm{tr}\mathbf{F}_2 - \mathrm{tr}\mathbf{F}_3\mathrm{tr}\mathbf{F}_4)\ [\mathbf{R},\mathbf{r}] = -\mathrm{tr}\mathbf{F}_5\ [\mathbf{R},\mathbf{r}] = -\gamma^{-6}p_1p_{21}\mathbf{F}, \tag{34}$$

where we used Eq.(42) to get $(\mathbf{rR}^2)^2 = U_1(z)\mathbf{rR}^2 - U_0(z)\mathbf{I} = \mathrm{tr}\mathbf{F}_3(\mathbf{rR}^2) - \mathbf{I}$, as well as Eqs.(31), (26), and (19). The roots of the Fibonacci spectral polynomial $p_{21}(E)$ determine the fifth order fragmentation pattern of the energy spectrum.

THE BASIC BLOCKS ALGEBRA

The main commutator expressions obtained in Sec. are summarized in Table I. Attending to their factorized forms the commutators listed in the third and fourth columns can be classified into two classes. On the one hand, we have those commutators which can be reduced to the simple expression

$$[\mathbf{B}_k,\mathbf{B}_l] = \pm\mathrm{tr}\mathbf{F}_j\ [\mathbf{R},\mathbf{r}] = \pm\gamma^{-(1+F_{j-1})}p_1p_{F_{j+2}}\mathbf{F}, \quad j \geq 1, \tag{35}$$

with $F_{j+2} = k + l - 3$. Eq.(35) shows that the emergence of successive fragmentation patterns in the energy spectrum, as prescribed by the roots of Fibonacci spectral polynomials $p_{F_j}(E)$, ultimately arises due to resonance effects among certain atomic clusters related to the blocks $\mathbf{B}_1 = \mathbf{r}$, $\mathbf{B}_2 = \mathbf{R}$, $\mathbf{B}_5 = \mathbf{RR}$, $\mathbf{B}_6 = \mathbf{rRr}$, $\mathbf{B}_7 = \mathbf{RrR} = \mathbf{F}_3$, $\mathbf{B}_9 = \mathbf{rRRr}$, and $\mathbf{B}_{17} = \mathbf{rRRrRRr}$, where the subscript indicates the number of bonds in the corresponding clusters. Accordingly, we will refer to these blocks as *basic* blocks thereafter. We note that 1) the elemental matrices $\mathbf{R}$ and $\mathbf{r}$ are included in the basic blocks set, and 2) the basic

block $\mathbf{B}_7$ belongs to the Fibonacci blocks family as well. At this point we should emphasize that the basic blocks listed in Table I are not the only possible blocking schemes able to give the simple factorized commutator form given by Eq.(35), but they are those involving the *minimum* number of elemental $\mathbf{R}$ and $\mathbf{r}$ matrices to this end. For instance, making use of the data listed in the first row of Table I along with Eq.(11), it is readily checked that $[\mathbf{rRRr},\mathbf{r}] = \mathbf{r}[\mathbf{RR},\mathbf{r}]\mathbf{r} = \mathrm{tr}\mathbf{F}_1[\mathbf{R},\mathbf{r}]$ or $[\mathbf{RrR},\mathbf{RR}] = -\mathbf{R}[\mathbf{RR},\mathbf{r}]\mathbf{R} = -\mathrm{tr}\mathbf{F}_1[\mathbf{R},\mathbf{r}]$, so that the simple commutator form $\mathrm{tr}\mathbf{F}_1[\mathbf{R},\mathbf{r}]$ can also be obtained by considering longer blocks, which naturally resolve in terms of the simpler $[\mathbf{RR},\mathbf{r}]$ commutator upon explicit calculation.

On the other hand, we have those commutators which include more than one Fibonacci block trace value in their factorized form:

$$[\mathbf{B}_k,\mathbf{B}_l] = \pm\prod \mathrm{tr}\mathbf{F}_j\ [\mathbf{R},\mathbf{r}] = \pm\gamma^{-(1+\hat{F}_j)}\prod p_{F_{j+2}}\mathbf{F}, \tag{36}$$

where $\hat{F}_j \equiv \max\{\mathrm{tr}\mathbf{F}_j\}$ and only certain Fibonacci blocks traces are included in the product, according to the selection rule $k+l-2 = \sum F_m$, where $\sum F_m$ stands for the sum of the Fibonacci spectral polynomials' degrees in Eq.(36).

Quite interestingly, factorized commutators given by Eqs.(35) and (36) can be written in the unified way

$$[\mathbf{B}_k,\mathbf{B}_l] = a_{kl}(U_j(z_i))[\mathbf{R},\mathbf{r}], \tag{37}$$

where $U_j(z_i)$ are Chebyshev polynomials of the second kind given in terms of Fibonacci blocks semi-traces $z_i = \frac{1}{2}\mathrm{tr}\mathbf{F}_i$, as is illustrated in Table II. Since these semi-traces can be readily expressed in terms of Fibonacci spectral polynomials $p_{Fj}(E)$, the tabulated factors a_{kl} are nested polynomials of the electron energy themselves.[50]

As a final remark we note that all the basic cluster blocks listed in Table I are palindromes, hence indicating that this symmetry has a fundamental significance in order to understand the energy spectrum structure of FQCs.[51] Indeed, according to a number of mathematical works published during the last two decades, palindromic order seems to play a fundamental role in the emergence of purely singular spectra in aperiodic systems based on the application of substitution rules.[52–55]

TRANSPORT PROPERTIES OF RESONANT STATES

The transport properties of electronic states in a given one-dimensional lattice can be studied by means of the Landauer conductance,[56] given by the expression $g_N(E) = g_0 T_N(E)$, where $g_0 = 2e^2/h$ is the quantum of conductance, and

$$T_N(E) = \frac{4(\det \mathcal{M}_N)^2 \sin^2 \kappa}{[M_{12} - M_{21} + (M_{11} - M_{22})\cos\kappa]^2 + (M_{11} + M_{22})^2 \sin^2 \kappa}, \tag{38}$$

is the transmission coefficient for a chain containing N atoms, where one assumes the lattice is sandwiched between two periodic chains (playing the role of contacts), each one with on-site energy ε' and transfer integral t', so that their dispersion relation is given by $E = \varepsilon' + 2t'\cos\kappa$. For the resonant energies given by Eq.(13) the global transfer matrix elements M_{ij} can be derived analytically

$$\mathcal{M}_N(E_*) = \mathbf{r}^{n_r}\,\mathbf{R}^{n_R} = \begin{pmatrix} U_N & -\gamma U_{N-1} \\ \gamma^{-1} U_{N-1} & -U_{N-2} \end{pmatrix}, \tag{39}$$

where $U_m(z)$ are Chebyshev polynomials of the second kind with $z = \frac{1}{2}\sqrt{E_*^2 - \epsilon^2} \equiv \cos\phi$.[3, 24, 32] Taking into account the relationship $U_m - U_{m-2} = 2T_m$, where $T_m(z) = \cos(m\cos^{-1} z)$ are Chebyshev polynomials of the first kind, one gets $|\mathrm{tr}(\mathcal{M}_N(E_*))| = |2\cos(N\phi)| \leq 2$, so that E_* belongs to the spectrum for any N value, and therefore in the quasiperiodic limit ($N \to \infty$) as well.

By plugging the M_{ij} elements given by Eq.(39), into Eq.(38) we obtain

$$T_N(E_*) = \left\{ 1 + \frac{(1-\gamma^2)^2}{(4 - E_*^2)\gamma^2} \sin^2 \left[N \cos^{-1}\left(\frac{\epsilon\gamma}{1-\gamma^2} \right) \right] \right\}^{-1}, \tag{40}$$

where $N \equiv F_j$ is a Fibonacci number, and we have assumed $\epsilon' = 0$ and $t' = 1$ for the sake of simplicity. As it can be readily seen, the transmission coefficient is always bounded below (i.e., $T_N(E_*) \neq 0$) for *any* lattice length, which proves the physically extended character of the E_* resonant states. Notwithstanding this, we must highlight that by extended we mean non-localized, and we do not necessarily have in mind a transparent, highly conductive state, as it occurs for Bloch states in periodic lattices. In fact, by systematically varying the adopted system length, the resulting transmission coefficients exhibit a series of alternating maxima (describing full transmission states with $T_N(E_*) = 1$) and minima (taking on values within the range $0 < T_N^{\min} < 1$), which correspond to those model parameters satisfying

pssb Macia.pdf

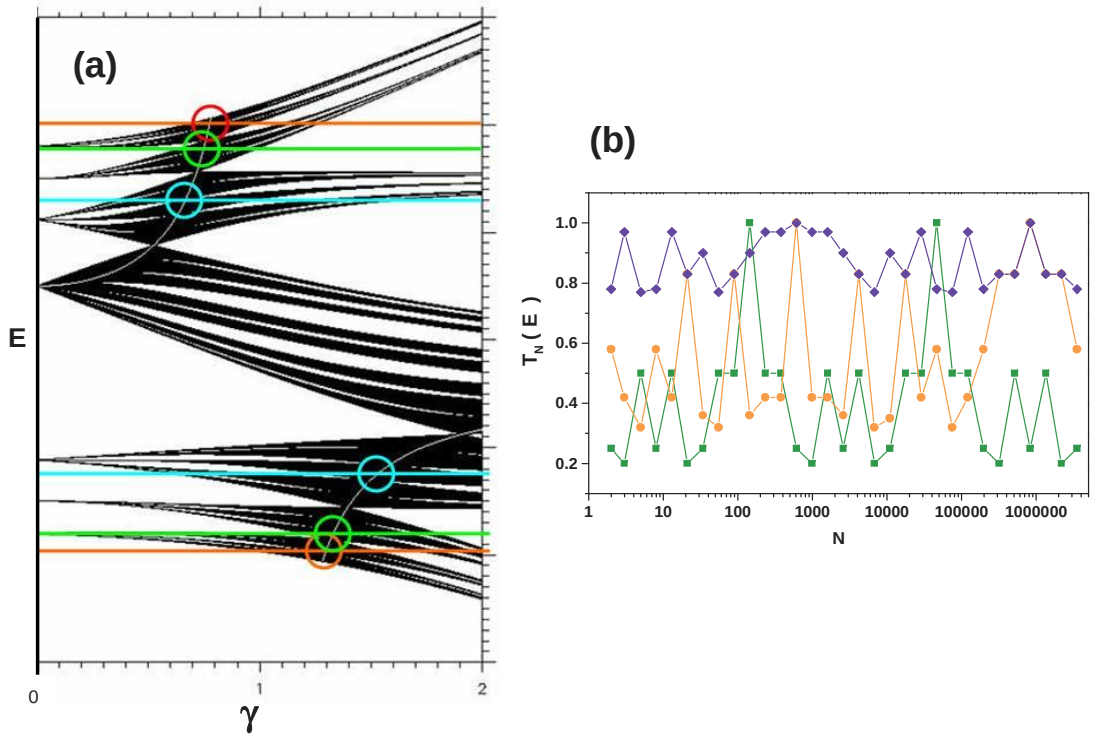

FIG. 5: (a) Numerically obtained phase diagram for the FQC shown in Fig.2, including the resonance energies $E^{(2)}_{\pm 2} = \pm\sqrt{13}/2$, $E^{+}_{\pm} = \pm\frac{\sqrt{11+2\sqrt{5}}}{2}$, and $E^{-}_{\pm} = \pm\frac{\sqrt{11-2\sqrt{5}}}{2}$, which are encircled in green, orange and blue, respectively. (b) Variation of the transport coefficients corresponding to the resonance energies $E^{(2)}_{\pm 2}$ (blue diamonds), $E^{+}_{\pm}$ (orange dots), and $E^{-}_{\pm}$ (green squares), encircled in Fig.5(a), as a function of the system size (ranging from $N = F_2 = 2$ to $N = F_{32} = 3524\,578$).

the conditions $\sin(N\phi) = 0$ and $\sin(N\phi) = 1$, respectively. Thus, the nature of the E_* extended states does not only include transparent states, typical of periodic systems, but also embraces a big set of states exhibiting a broad palette of possible Landauer conductance values, ranging from highly conductive to highly resistive ones.

For the sake of illustration in Fig.5(b) we plot the transmission coefficients corresponding to the resonance energies encircled in Fig.5(a) as a function of the number of atoms in the FQC. These energies correspond to the crossing points between the zeroth-order energy

curve and the first- and second-order energy spectra bands, respectively. The coordinates for the zeroth-first order bands crossing points in the phase diagram were previously obtained and its location is shown in Fig.3 for the particular model parameters choice $\epsilon = 1/2$ and $N = 34$. The coordinates for the zeroth-second order bands crossing points can be analytically obtained from the condition $p_5(E_*, \epsilon, \gamma) = 0$, and they are given by the general expressions

$$\gamma_{\pm}^{+} = \sqrt{1 + b_{+}\left(1 \pm \sqrt{1 + \frac{2}{b_{+}}}\right)}, \quad \gamma_{\pm}^{-} = \sqrt{1 + b_{-}\left(1 \pm \sqrt{1 + \frac{2}{b_{-}}}\right)},$$
$$E_{\pm}^{+} = \pm\sqrt{\epsilon^2 + \tau^2 + 1}, \quad E_{\pm}^{-} = \pm\sqrt{\epsilon^2 + 3 - \tau},$$

where $b_{\pm} \equiv \frac{\epsilon^2}{2a_{\pm}}$, with $a_{\pm} = \frac{5 \pm \sqrt{5}}{8}$, and $\tau \equiv \frac{1+\sqrt{5}}{2}$ is the golden mean.

Two main conclusions can be drawn from Fig.5. First, the Landauer conductance of these resonant states sensitively depends on the number of atoms in the considered FQC, exhibiting a remarkable log-periodic pattern which is characteristic of each energy value. This log-periodic feature stems from an interesting relationship between the Fibonacci number $N = F_j$ value and its related divisors.[57] Second, the Landauer conductance variation range depends on the relative location of the considered resonant state in the overall energy spectrum, taking on significantly higher (lower) $T_N^{\min}$ values for eigenvalues located closer to the less (more) fragmented regions of the spectrum, respectively. In addition, we note that the resonance energies $E_{\pm}^{+} \simeq \pm 1.966\,731\ldots$ (which are close to the energy spectrum band-edges located at $E_*^{\rm b} = \pm\sqrt{\epsilon^2 + 4\cos^2\left(\frac{\pi}{2N}\right)} = \pm 2.059482\ldots$ for the model parameters choice $\epsilon = 1/2$ and $N = 34$) exhibit relatively high conductance values (including full transmission ones for some specific N values), in agreement with the experimental results obtained in the study of light transport through the band edge states of photonic FQCs.[58, 59]

CONCLUSIONS

The dynamics of electrons in FQCs is conveniently described in terms of suitable block matrices, say $\mathbf{B}_k$, involving a number of elemental matrices $\mathbf{r}$ and $\mathbf{R}$. These block matrices characterize certain local arrangements of atoms and bonds (clusters) whose resonance energies can be properly obtained by means of commutators of the form $[\mathbf{B}_k, \mathbf{B}_l]$. These commutators naturally introduce a correlation length allowing for the onset of multiple res-

onance effects at different scales, which give rise to a nested hierarchy of splitting patterns in the energy spectrum. The full-fledged overall spectrum structure is then determined by local scale resonances involving locally isomorphic atomic clusters of progressively increasing sizes. In this way, we disclose a full hierarchy of resonant states naturally related to the quasiperiodic long-range order of FQCs. *The transmission coefficient of these resonant states is always bounded below, although their related Landauer conductance values may range from highly conductive to highly resistive ones, depending on the number of atoms in the considered FQC.*

The recourse to basic cluster blocks allows one to readily disclose suitable blocking schemes yielding commutators which can be readily factorized in terms of Fibonacci spectral polynomials. In this way, we can classify the resonance energies defining the different fragmentation patterns of the energy spectrum on the basis of purely algebraic criteria. This feature significantly contributes to gain a better understanding of the symmetry principles governing the fragmentation process of the energy spectrum in a clear way. Thus, the overall electronic energy spectrum of an arbitrary FQC of length $N = F_j$, can be obtained as a superposition of an increasing number of bi-parametric resonance energy curves $E = E_{F_j}(\epsilon, \gamma)$ obtained from the roots of a hierarchical series of spectral Fibonacci polynomials $p_{F_j}(E)$. In so doing, we are able to disclose the physical role played by different kinds of symmetries naturally intertwined in FQCs, namely, the inflation/deflation global symmetry described by the characteristic Fibonacci substitution rule g, the repetitiveness symmetry related to the local isomorphism property and palindromicity.

APPENDIX

The Cayley-Hamilton theorem states that any $n \times n$ square matrix $\mathbf{M}$ over the real or complex field is a root of its own characteristic polynomial $\det(\mathbf{M}-\lambda\mathbf{I}) = 0$,[49] so that one can write

$$\mathbf{M}^2 - 2z\mathbf{M} + \mathbf{I}\det\mathbf{M} = \mathbf{0}, \tag{41}$$

where $z \equiv \frac{1}{2}\mathrm{tr}\mathbf{M}$. If $\mathbf{M}$ belongs to the $SL(n,\mathbb{R})$ group one can readily use (41) in order to properly express any higher power of $\mathbf{M}$ as a linear combination of matrices $\mathbf{I}$ and $\mathbf{M}$. In the case of 2×2 unimodular matrices one obtains by induction the expression

$$\mathbf{M}^N = U_{N-1}(z)\mathbf{M}-U_{N-2}(z)\mathbf{I}, \tag{42}$$

where

$$U_N \equiv \frac{\sin(N+1)\varphi}{\sin\varphi}, \tag{43}$$

with $\varphi \equiv \cos^{-1} z$, are Chebyshev polynomials of the second kind satisfying the recursion relation

$$U_{k+1} - 2zU_k + U_{k-1} = 0, \quad k \geq 1 \tag{44}$$

with $U_0(z) = 1$ and $U_1(z) = 2z$.

Let $\mathbf{A}$ and $\mathbf{B}$ be 2×2 unimodular matrices. According to the Cayley-Hamilton theorem we have

$$(\mathbf{AB})^2 = U_1(z)\mathbf{AB} - U_0(z)\mathbf{I}, \; (\mathbf{BA})^2 = U_1(z)\mathbf{BA} - U_0(z)\mathbf{I}, \tag{45}$$

with $U_1(z) = \mathrm{tr}(\mathbf{AB}) = \mathrm{tr}(\mathbf{BA})$. Making use of (45) we readily obtain the useful relation

$$[\mathbf{BAB}, \mathbf{A}] = -U_1(z)[\mathbf{A}, \mathbf{B}] = -\mathrm{tr}(\mathbf{AB})[\mathbf{A}, \mathbf{B}]. \tag{46}$$

ACKNOWLEDGEMENTS

I warmly thank Prof. Roland Ketzmerick for sharing useful materials and M. Victoria Hernández for a critical reading of the manuscript.

[1] Z. M. Stadnik, Ed *Physical Properties of Quasicrystals*; Springer Series in Solid-State Physics Vol. **126**; **(**Springer, Berlin, 1999)

[2] J. M. Dubois, *Useful Quasicrystals* (World Scientific, 2005)

[3] E. Maciá Barber, *Aperiodic Structures in Condensed Matter* (CRC Taylor & Francis, Boca Raton, 2009) Chapter 3

[4] J. M. Dubois and E. Belin-Ferré, *Introduction to the science of complex metallic alloys* in *Complex Metallic Alloys. Fundamentals and Applications*, J. M. Dubois and E. Belin-Ferré, eds; Wiley-VCH, Weinheim (2011); p.1.

[5] A. Prekul and N. Shchegolikhina, Crystals 2016, 6, 119; doi:10.3390/cryst6090119.

[6] K. Kirihara, T. Nagata, K. Kimura, K. Kato, M. Takata, E. Nishibori, and M. Sakata, Phys. Rev. B **68**, 014205 (2003).

[7] M. Krajčí and J Hafner, J. Phys. Condens. Matter, **14**, 1865 (2002).

[8] G. Trambly de Laissardière, D. Nguyen-Manh, and D. Mayou, J. Non-Cryst. Solids, **334&335**, 347 (2004).

[9] Y. Takagiwa and K. Kirihara, Sci. Technol. Adv. Mater, **15**, 044802, 2014.

[10] H.Sato, T. Takeuchi, and U. Mizutani, Phys. Rev. B **64,** 094207 (2001).

[11] J. Dolinšek and A. Smontara, Isr. J. Chem. **51**, 1246 (2011).

[12] Q. Niu and F. Nori, Phys. Rev. Lett. **57**, 2057 (1986).

[13] Q. Niu and F. Nori, Phys. Rev. B **42**, 10329 (1990).

[14] V. Sánchez and C. Wang, Phys. Rev. B **70,** 144207 (2004).

[15] S. Thiem and M. Schreiber, Phys. Rev. B **85**, 224205 (2012).

[16] S. Thiem and M. Schreiber, J. Phys. Condens. Matt. **25** 075503 (2013).

[17] F. Sánchez, V. Sánchez, and C. Wang, Physica B, **449**, 121 (2014).

[18] C. Wang, C. Ramírez, F. Sánchez, and V. Sánchez, Phys. Status Solidi B **252**, 1370 (2015).

[19] F. Sánchez, V. Sánchez, and C. Wang, J. Non-Cryst. Solids **450**, 194 (2016).

[20] V. Kumar, J. Phys. Condens. Matt. **2**, 1349 (1990).

[21] A. Chakrabarti and S. N. Karmakar, Phys. Rev. B **44**, 896 (1991).

[22] A. Chakrabarti, S. N. Karmakar and R. K. Moitra, Phys. Lett. A **168**, 301 (1992).

[23] A. Chakrabarti, S. N. Karmakar and R. K. Moitra, Phys. Rev. B **50**, 13276 (1994).

[24] E. Maciá and F. Domínguez-Adame, Phys. Rev. Lett. **76**, 2957 (1996).

[25] A. Ghosh and S. N. Karmakar, Phys. Rev. B **58**, 2586 (1998).

[26] V. Sánchez, L. A. Pérez, R. Oviedo-Roa, and C. Wang, Phys. Rev. B **64,** 174205 (2001).

[27] S. Chattopadhyay and A. Chakrabarti, Phys. Rev. B **65**, 184204 (2002).

[28] E. L. Albuquerque and M. G. Cottam, Phys. Rep. **376**, 225 (2003).

[29] U. Grimm, Isr. J. Chem. **51**, 1257 (2011).

[30] D. Damanik, M. Embree, and A. Gorodetski, Spectral properties of Schrödinger operators arising in the study of quasicrystals, Prog. Math. Phys. **309**, 307-370, in *Mathematics of Aperiodic Order*, J. Kellendonk, D. Lenz, J. Savinien (eds.) (Springer, Berlin, 2015).

[31] D. Damanik, A. Gorodetski, and W. Yessen, Invent. Math. **206**, 629 (2016).

[32] E. Maciá, ISRN Condensed Matter Physics **2014**, 165943 (2014). doi: 10.1155/2014/165943.

[33] E. Maciá, Phys. Rev. B **60**, 10032 (1999).

[34] E. Maciá, Phys. Rev. B **61** 6645 (2000).

[35] W. Yessen, J. Spectr. Theory **3**, 101 (2013).

[36] We note that the term *Fibonacci quasicrystal* has also been used in the literature to refer to the models which are not described in terms of a tridiagonal Hamiltonian.

[37] We note that these overlapping molecules play a role similar to that played by overlapping atomic clusters in the structural models proposed for the binary icosahedral quasicrystal $Cd_{85}Yb_{15}$, as discussed in H. Takakura, C. Pay-Gómez, A.Yamamoto, M. de Boissieu and A. P. Tsai, Nature Materials **6**, 58 (2007). See also, W. Steurer and S. Deloudi, *Crystallography of Quasicrystals - Concepts, Methods and Structures*, Springer Series in Materials Science 126 (Springer Verlag, Berlin, 2009), p.300-305.

[38] M. Mei and W. Yessen, Math. Model Nat. Phenom. **9**, 204 (2014).

[39] M. Kohmoto, L. P. Kadanoff, and C. Tang, Phys. Rev. Lett. **50**, 1870 (1983).

[40] S. Ostlund, R. Pandit, D. Rand, H. J. Schellnhuber, and E. D. Siggia, Phys. Rev. Lett. **50** 1873 (1983).

[41] We note that these atomic clusters do not coincide with those previously introduced in Sec. (see Fig.1) since a deflation process is an exact symmetry operation which does not allow for overlapping between neighboring clusters.

[42] Recently, a decomposition scheme based on the mirror symmetric AB and AAB molecules has been exploited in order to study the dynamics of classical particles in a time-driven Fibonacci lattice, as discussed in T. Wolf and P. Schmelcher, Phys. Rev. E **93**, 042215 (2016).

[43] Alternatively, making use of the concatenation formula $\tilde{\mathbf{F}}_n = \tilde{\mathbf{F}}_{n-2}\tilde{\mathbf{F}}_{n-1}$, $n \geq 2$, starting with $\tilde{\mathbf{F}}_0 \equiv \mathbf{r}$, $\tilde{\mathbf{F}}_1 \equiv \mathbf{R}$, we can obtain completely analogous expressions to those given by Eqs.(6)-(8) and (12).

[44] A. Bovier and J. M. Ghez, J. Phys. A: Math. Gen. **28,** 2313 (1995).

[45] Rather it belongs to the Lie algebra $sl(2,\mathbb{R})$, naturally related to the $SL(2,\mathbb{R})$ Lie group. See, for instance, P. H. Sattiger and O. L. Weaver, *Lie Groups and Algebras with Applications to Physics, Geometry and Mechanics* (University of Bangalore Press, Bangalore, 1997).

[46] M. Kohmoto, B. Sutherland, and C. Tang, Phys. Rev. B **35**, 1020 (1987).

[47] Completely analogous expressions are similarly obtained for the traces of Fibonacci blocks $\tilde{\mathbf{F}}_n$.

[48] For convenience, we introduce the notation $E_j^{(n)}$ for the Fibonacci spectral polynomials roots, where n labels the fragmentation order of the considered energy spectrum.

[49] F. R. Gantmacher, *The Theory of Matrices* **2** (Chelsea, New York, 1974).

[50] As it was discussed in E. Maciá, Phys. Rev. B **73**, 184303 (2006) this nested structure allows

one to obtain information regarding the corresponding dispersion relation in a closed way.

[51] C. Morfonios, P. Schmelcher, P. A. Kalozoumis, and F. K. Diakonos, Nonlinear. Dyn. **78**, 71 (2014).

[52] A. Hof, O. Knill, and B. Simon, Comm. Math. Phys. **174**, 149 (1995).

[53] M. Baake, Lett. Math. Phys. **49**, 217 (1999).

[54] J. P. Allouche, M. Baake, J. Cassaigne, and D. Damanik, Theoret. Comput. Sci. **292**, 9 (2003).

[55] S. Labbé and E. Pelantová, Eur. J. Combin. **51,** 200 (2016).

[56] Y. Imry and R. Landauer, Rev. Mod. Phys. **71**, S306 (1999).

[57] X. Huang and C. Gong C, Phys. Rev. B **58** 739 (1998).

[58] L. Dal Negro, C. J. Oton, Z. Gaburro, L. Pavesi, P. Johnson, A. Lagendijk, R. Righini, M. Colocci, and D. S. Wiersma, Phys. Rev. Lett. **90**, 055501 (2003).

[59] M. Ghulinyan, C. J. Oton, L. Dal Negro, L. Pavesi, R. Sapienza, M. Colocci, and D. S. Wiersma, Phys. Rev. B **71**, 094204 (2005).

$\mathbf{B}_k$	$\mathbf{B}_l$	$[\mathbf{B}_k, \mathbf{B}_l]$	$[\mathbf{B}_k, \mathbf{B}_l]$
RR	**r**	$\mathrm{tr}\mathbf{F}_1[\mathbf{R}, \mathbf{r}]$	$\gamma^{-2}p_1p_3\mathbf{F}$
RrR	**r**	$\mathrm{tr}\mathbf{F}_2[\mathbf{R}, \mathbf{r}]$	$\gamma^{-2}p_1p_5\mathbf{F}$
rRr	**R**	$-\mathrm{tr}\mathbf{F}_2[\mathbf{R}, \mathbf{r}]$	$-\gamma^{-2}p_1p_5\mathbf{F}$
rRRr	**R**	$-\mathrm{tr}\mathbf{F}_3[\mathbf{R}, \mathbf{r}]$	$-\gamma^{-3}p_1p_8\mathbf{F}$
rRRr	**RrR**	$-\mathrm{tr}\mathbf{F}_4[\mathbf{R}, \mathbf{r}]$	$-\gamma^{-4}p_1p_{13}\mathbf{F}$
rRRrRRr	**RrR**	$-\mathrm{tr}\mathbf{F}_5[\mathbf{R}, \mathbf{r}]$	$-\gamma^{-6}p_1p_{21}\mathbf{F}$
rRr	**RR**	$-\mathrm{tr}\mathbf{F}_1\mathrm{tr}\mathbf{F}_2[\mathbf{R}, \mathbf{r}]$	$-\gamma^{-3}p_1p_3p_5\mathbf{F}$
rRRr	**RR**	$-\mathrm{tr}\mathbf{F}_1\mathrm{tr}\mathbf{F}_3[\mathbf{R}, \mathbf{r}]$	$-\gamma^{-4}p_1p_3p_8\mathbf{F}$
RrRRrR	**rRRr**	$\mathrm{tr}\mathbf{F}_3\mathrm{tr}\mathbf{F}_4[\mathbf{R}, \mathbf{r}]$	$\gamma^{-6}p_1p_8p_{13}\mathbf{F}$
RRrRrRR	**rRr**	$-\mathrm{tr}\mathbf{F}_1\mathrm{tr}\mathbf{F}_2\mathrm{tr}\mathbf{F}_4[\mathbf{R}, \mathbf{r}]$	$-\gamma^{-6}p_1p_3p_5p_{13}\mathbf{F}$

TABLE I: Basic blocks and their related commutator expressions. Some commutators listed in this Table can be obtained making use of Eq.(46). For instance, we have $[\mathbf{RRrRrRR}, \mathbf{rRr}] = [\mathbf{B}_6\mathbf{B}_7\mathbf{B}_6] = -\mathrm{tr}(\mathbf{B}_7\mathbf{B}_6)[\mathbf{B}_7, \mathbf{B}_6] = -\mathrm{tr}\mathbf{F}_4[\mathbf{B}_7, \mathbf{B}_6] = -\mathrm{tr}\mathbf{F}_1\mathrm{tr}\mathbf{F}_2\mathrm{tr}\mathbf{F}_4[\mathbf{R}, \mathbf{r}]$, where we used the cyclic property $\mathrm{tr}(\mathbf{rRrRR}) = \mathrm{tr}(\mathbf{RrRRr}) = \mathrm{tr}\mathbf{F}_4$. Note that all basic block are palindromes.

a_{kl}	B_1	B_2	B_5	B_6	B_7	B_9	B_{17}
B_1	0	-1	$-U_1(z_1)$	-1	$-U_1(z_2)$	$-U_1(z_1)$	$-U_1(z_1)U_1(z_3)$
B_2	1	0	0	$U_1(z_2)$	1	$U_1(z_3)$	$U_2(z_3)$
B_5	$U_1(z_1)$	0	0	$U_1(z_1)U_1(z_2)$	$U_1(z_1)$	$U_1(z_1)U_1(z_3)$	$U_1(z_1)U_2(z_3)$
B_6	1	$-U_1(z_2)$	$-U_1(z_1)U_1(z_2)$	0	$-U_2(z_2)$	$U_1(z_0)$	$U_1(z_0)U_1(z_3) - 1$
B_7	$U_1(z_2)$	-1	$-U_1(z_1)$	$U_2(z_2)$	0	$U_1(z_4)$	$U_1(z_5)$
B_9	$U_1(z_1)$	$-U_1(z_3)$	$-U_1(z_1)U_1(z_3)$	$-U_1(z_0)$	$-U_1(z_4)$	0	$-U_1(z_1)$
B_{17}	$U_1(z_1)U_1(z_3)$	$-U_2(z_3)$	$-U_1(z_1)U_2(z_3)$	$1 - U_1(z_0)U_1(z_3)$	$-U_1(z_5)$	$U_1(z_1)$	0

TABLE II: Matrix representation of the trace factors related to the basic blocks commutators set. The commutators properties $[\mathbf{B}_i, \mathbf{B}_i] = 0$ and $[\mathbf{B}_j, \mathbf{B}_i] = -[\mathbf{B}_i, \mathbf{B}_i]$ guarantee that this matrix belongs to the Lie algebra $sl(2, \mathbb{R})$.